CHAPTER 1

Introduction to MRI

The story of Magnetic Resonance Imaging (MRI) begins with the nuclear magnetic resonance phenomenon, discovered just before and during the Second World War. The technique was refined over the ensuing decades, and a multitude of experimental and theoretical studies were devised to explore the factors that affected the precise magnetic resonance frequencies at which nuclei resonate in a strong external field. A key revelation was that even slight differences in the molecular environments of the nuclei cause detectable shifts in their behaviors. Researchers realized that such studies, especially when in combination with x-ray diffraction results, could be invaluable in unraveling molecular structures. Also of great importance, it became possible to explain the associated nuclear-spin relaxation (T1, T2) mechanisms, which would come to play so central a clinical role in MRI.

In the mid-1970s, scientists designed methods to carry out NMR voxel-by-voxel within a thin slice of tissue, thereby enabling the delineation of two-dimensional MRI maps of T1 and of T2 throughout the body. This led to further approaches—such as *MR spectroscopy* (MRS), *functional MRI* (fMRI), *diffusion tensor imaging* (DTI), and *MR angiography* (MRA)—that portray the spatial dependences of other physiological and metabolic tissue properties, too. All of this has established MRI as a powerful and extraordinarily versatile diagnostic modality with a number of unique imaging capabilities. Were it not for their still significantly greater cost, MRI machines might well drive CT largely out of business.

This chapter will say a bit about NMR and MRI in general, then illustrate some of the remarkable capabilities of MRI with a real case study.

There follows a sketch of the rich history of the field, and an important caveat: there are potentially lethal but preventable hazards associated with strong and rapidly switching magnetic fields and with the intense pulses of radiofrequency (RF) energy from an MR device. Be careful for yourself, your patients, and all others.

1.1 A Stratospheric, Warp-Speed View of NMR and MRI

This brief section zip-lines through much of the physics of NMR and MRI. We shall provide only cursory descriptions now, but you can expect the explanations and fuller descriptions to follow in the rest of the book. Many of the whys and wherefores may not be apparent here, but they will come later.

The nuclear magnetic moment is proportional to the nuclear spin

The normal chemical properties of virtually any atom are determined solely by the arrangement of its electrons, hence ultimately by the number of protons in the nucleus, the atomic number, Z. Gases, liquids, solids, and living cells behave the way they do because of, and almost only because of, the configurations of the Z electrons of their constituent atoms.

The properties of a nucleus itself, however, depend on the number of neutrons, N, as well. The values of both Z and N together govern whether or not a specific isotope is radioactive, of importance in nuclear medicine, and in the cleanup of nuclear power reactors and weapons facilities. The makeup of a nucleus also determines its magnetic properties, which are fundamental to MRI. It can be fruitful to think of a nucleus as being somewhat like a spinning ball of positive charge [Eisberg et al. 1985]. A proton, a neutron, or a composite nucleus has a quantum mechanical (QM) attribute that is called, by analogy with the corresponding vector property of classical physics, *nuclear spin angular momentum*, $\boldsymbol{I}$, or just spin, as in Figure 1.1.

The only nucleus currently of major interest in clinical MRI is the simplest of them all, namely that of an atom of ordinary hydrogen, i.e., a solitary proton. A nuclear physicist views a proton as a subatomic particle made up of two up-quarks and one down-quark held together by the strong nuclear force. Just as interactions among charged particles are brought about by the virtual photons of quantum electrodynamics, likewise quarks are bound by the virtual gluons of chromodynamics, within a sea of virtual quarks that are constantly appearing and vanishing. Mother Nature has

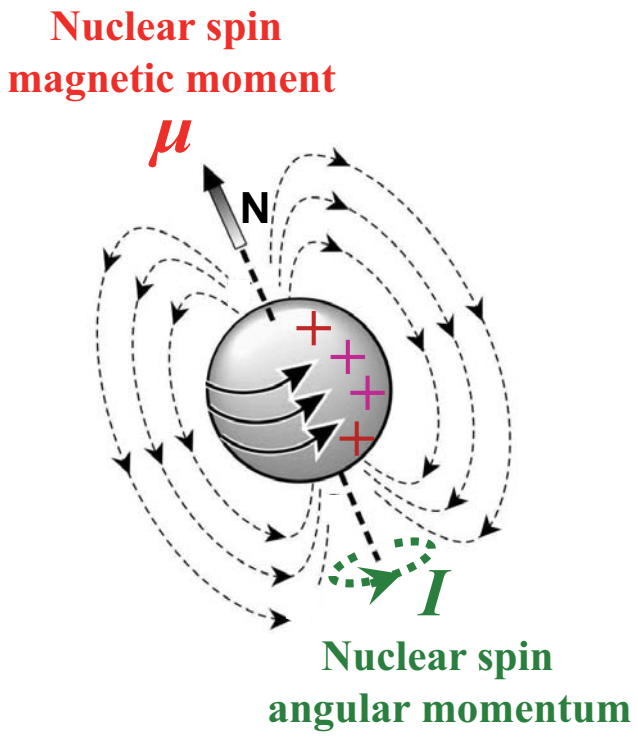

Figure 1.1 A free nucleus has a quantum mechanical attribute analogous to classical spin and is said to possess *spin angular momentum, S*. As a 'spinning' charged body, it produces its own weak magnetic field, like that of a compass needle or small bar magnet. The strength of this nuclear magnet is parameterized by its nuclear spin magnetic moment, represented as the vector quantity $\boldsymbol{\mu}_n$, of magnitude $\mu_n \equiv |\boldsymbol{\mu}_n|$.

decreed that, despite the problems theorists are having in getting the spins of its quarks and gluons to add up right (a situation known as the 'proton spin crisis'), a lone proton is one of many nuclei considered to be a 'spin-½' particle, therefore a fermion.

Every nucleus comprised of an odd number of protons or of neutrons or both possesses non-zero spin. In any nucleus with even numbers of both protons and neutrons, at the other extreme, each proton pairs up and aligns anti-parallel to another, for reasons that can be explained with QM, and their two dipole magnetic fields cancel—they have zero net spin. The same is also true of the neutrons. As a result, carbon-12, oxygen-16 (which, together with hydrogen, make up ¾ of the mass of soft tissues), and calcium-40 play no active role in imaging.

As with any other charged and moving entity, a 'spinning' nucleus produces its own magnetic *dipole* field, its *nuclear magnetic moment*, a vector entity that is represented by a lower-case italic Greek mu, $\boldsymbol{\mu}$. The magnitude or strength of the inherent nuclear moment of the n^{th} isotope, designated $\mu_n \equiv |\boldsymbol{\mu}_n|$, is a principal measure of its 'magnetness,' the strength of the field it itself produces.

The *gyromagnetic ratio*, γ_n, is a slightly different measure of the same thing, the strength of the intrinsic nuclear magnetic field of the nucleus. Encountered more commonly as $(\gamma_n/2\pi)$, it relates the nuclear magnetic moment to the nuclear spin angular momentum vector, $\boldsymbol{I}_n$,

$$\boldsymbol{\mu}_n = \gamma_n \boldsymbol{I}_n \tag{1.1a}$$

At times it is more convenient to use $\gamma_n/2\pi$ rather than μ_n in discussion, or vice versa, but otherwise the two are equivalent, apart from a constant.

The subscripts on I_n, μ_n, and γ_n label specific nuclear isotopes by their atomic weight,

$$n \equiv (Z_n + N_n). \tag{1.1b}$$

Clinical MRI deals almost exclusively with the nuclei of regular hydrogen atoms, $^1H_1$ or H-1 in the standard notation, so there is no further need for the subscript, and the magnitudes of the two vectors can be related as

$$\boldsymbol{\mu} = \gamma \boldsymbol{I} \tag{1.1c}$$

The protons that are imaged are found almost entirely in cellular or extra-cellular water or lipids and, again, we shall refer to them generally as *tissue protons*. So hereafter, γ and μ will appear unadorned with an 'n,' and they will refer only to hydrogen nuclei in tissues.

From here, traditional introductions to NMR and MRI physics take one of two pedagogic paths, the quasi-quantum 'spin-up/spin down' and the 'classical.' We shall, however, be guided by the incontrovertible wisdom of Yogi Berra, philosopher and former catcher for the resplendent New York Yankees: "If you come to a fork in the road, take it." Both routes happened to pass by his house, and such is the case here, too.

Some Notes on Vectors

Before proceeding with our story, we should clarify the notation for vectors. A magnetic field, $\boldsymbol{B}$, which has both magnitude and direction, is a *vector* entity and is represented with a **bolded** symbol. Its strength, B, a scalar, is not in bold. $\boldsymbol{B}(\boldsymbol{r})$ is a *vector field* that has magnitude or direction that may vary according to the value of the position vector $\boldsymbol{r}$. We shall deal frequently with the particular one-dimensional situation of a 1D patient reposing along the *x-axis* and in an external field whose strength varies with *x—but that always points along the z-axis*! This might be written $\boldsymbol{B}(x)$, but when it is necessary to emphasize the fixed direction of the external field, it will be presented as $\boldsymbol{B}_z(x)$.

Individual components of a vector will *not* be denoted in bold: for example, x is the first spatial component of the three-space position vector $\boldsymbol{r} \equiv \{x,y,z\} = x\mathbf{i} + y\mathbf{j} + z\mathbf{k}$, where **i**, **j**, and **k** are the orthonormal unit vectors of 'real-' or 'three-' space. This may also be expressed as $\boldsymbol{r} \equiv \{x_1, x_2, x_3\} = x_1\mathbf{i} + x_2\mathbf{j} + x_3\mathbf{k}$.

In mathematics and computer science, on the other hand, some quantities with multiple, discrete values can be treated as vectors or arrays, such as with the vector $\boldsymbol{x} \equiv \{x_1, x_2, x_3, \ldots, x_n\}$ that specifies the positions of voxels 1, 2, …, n along the x-axis of an image. We shall *not* denote the individual members of this set as vectors with bold font.

Similarly, when discussing the rather enigmatic construct known as $\boldsymbol{k}$-space, $\boldsymbol{k} \equiv \{k_x, k_y, k_z\}$ (which is totally, absolutely *not* related to the unit **k**-vector of real-space) will represent a single vector location in that space.

Every concept introduced briefly in this chapter, by the way, will be pursued more fully later on.

First picture of NMR: Quasi-quantum mechanical (spin-up/spin-down along B_z and the z-axis)

The easier way to begin addressing proton NMR is by way of a great simplification of the full quantum mechanical (QM) treatment.

Imagine that in a magnetically shielded room, a tray of compasses is being mechanically rattled gently. With no external magnetic field, their needles are jostled about and randomly point in all directions because of the effects of the 'noise' energy being inputted. When a strong external field, $\boldsymbol{B}_z$, is present, however, then the needles will tend to align relative to it, each with its own north pole heading toward the magnet's

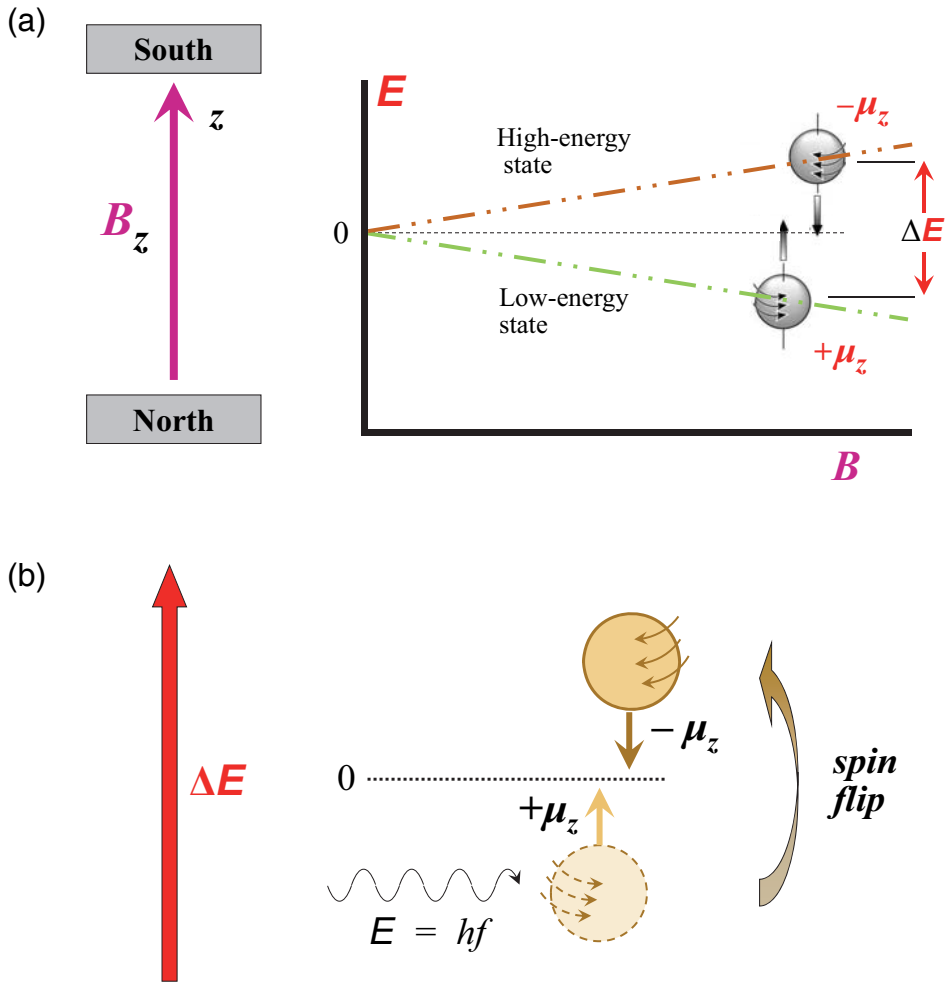

Figure 1.2 There are two pedagogical pictures of NMR, the *quasi-QM* and the *classical*, that are commonly drawn upon in introducing MRI physics. The two are mutually incompatible and inconsistent, and they cannot be combined together, because of the quite different assumptions adopted in constructing each of them out of the fully correct, rigorous quantum theory. But both are useful in different ways. Here we discuss only the greatly simplified *quasi-QM* picture. (a) A single proton behaves like a tiny compass needle, but it can align in an externally magnetic field, $\boldsymbol{B}_z$, *only along* or *against* it and the **z**-axis. The energy levels for the two quasi-QM proton spin states diverge by the amount of the Zeeman energy, which is linear in the strength of the total local magnetic field. Nearly all of this $\boldsymbol{B}_z$ comes from the main magnet, and is constant. Much of the rest is from the intermittently activated *gradient coils*, and from the brief pulses from the RF (radiofrequency) *transmitter*. Finally, the amount of random RF 'noise' generated by fluctuations in molecular motions is tiny, but it greatly influences proton spin relaxation processes. A spin-½ nucleus such as a proton is allowed to inhabit either one of the two levels: in the lower-energy, 'spin-up' state, the projection of $\boldsymbol{\mu}$ onto the **z**-axis is aligned parallel to $\boldsymbol{B}_z$. Alternatively, in the 'down,' high-energy state, it points against $\boldsymbol{B}_z$. Also, *un*like a compass needle, a proton can remain for long periods of time in a quasi-stable, higher-energy spin-orientation state, pointing the 'wrong' direction. (b) The two spin states differ by the Zeeman energy, $\Delta E = 2\mu_z \boldsymbol{B}_z$. A photon (or phonon) of the right energy can cause a transition up or down between the two. The horizontal dashed line in the middle indicates the energy the nucleus has at $\boldsymbol{B}_z = 0$.

south pole. But by grabbing and twisting a needle you can make it point in any direction you choose, until you let it go.

Protons behave only somewhat like that. When a bunch of them are inserted into the uniform field $\boldsymbol{B}_z$, they will be *polarized*, but—as it happens, perhaps somewhat mysteriously—with only half of them aligned *along* it and the other half *against*. This is a wonderful example of what is affectionately known as *quantum weirdness*. The spin magnetic moment of a proton is *spatially quantized*, and its z-component can align only 'up' along the direction of the external field or 'down' against it. According to this simplified, quasi-QM picture, the nucleus can exist in either of these two possible spin states in the external field—and, *un*like a compass needle, with no other alignments (Figure 1.2a). In other words, the *z-components* of a proton's nuclear magnetic moment can assume only the values

$$\mu_z = \pm\tfrac{1}{2}(h/2\pi)\gamma \qquad (1.1d)$$

If the field produced by the nucleus itself aligns *along* an external field, as with a compass needle, then the nucleus is said to inhabit the *lower-energy*, or *spin-up*, state.

It simplifies many of the illustrations in this book to align the main external field vertically, somewhat like the energy scale. While the fields of superconducting magnets are mostly horizontal, those of permanent and electromagnets are vertical, so there's nothing really to unlearn to assume, for now, that they point upward.

The classical *energy of alignment* of a magnetic dipole moment in a z-orientated external field is given by the vector *dot* (or *scalar*) product

$$E = \boldsymbol{\mu} \cdot \boldsymbol{B}_z, \qquad (1.2a)$$

and this general form remains valid quantum mechanically. To avoid confusion with the electric field $\boldsymbol{E}$, the E intended to represent the non-vector *energy* is shown in Arial typeface. From Equations (1.1) and (1.2a), the QM *Zeeman splitting*, ΔE_{Zeeman}, between the two energy levels of a spin-½ nucleus, is proportional both to its innate magnetness (μ or γ) and to the strength of the local magnetic field there, $\boldsymbol{B}_z$:

$$\Delta E_{Zeeman} = 2\mu_z B_z = h(\gamma/2\pi)B_z. \qquad (1.2b)$$

EXERCISE 1.1 What are the units of μ?

At the heart of MRI is the critical fact that a proton in its lower-energy spin state can be elevated to a high-energy state by interaction with an applied radiofrequency photon that carries exactly the right energy. Indeed, one easy way to determine that the *nuclear magnetic resonance* process is occurring in a sample of water, say, is to turn on an external magnetic field $\boldsymbol{B}$, pass a beam of RF photons through it, and detect the rate at which it absorbs the energy as a function of the frequency, v. Bearing in mind the ubiquitous Planck-Einstein relationship between the energy of a photon and its frequency, $E = hv$, then the energy required to flip over a proton in the field $\boldsymbol{B}_z$ is

$$\boxed{hv = \Delta E_{Zeeman} = h(\gamma/2\pi)B_z,} \quad \text{or} \quad \boxed{v_{Larmor}(B_z) = (\gamma/2\pi)B_z.} \qquad (1.2c)$$

This is the central *Larmor equation*, which relates the frequency at which a cohort of protons gathered together in a magnetic field of local magnitude B_z will undergo the phenomenon of nuclear magnetic resonance. NMR is one of the two essential concepts of MRI (the other being *spin-relaxation*), and here you are at only page 5! Imagine how much more you'll pick up in the rest of the book.

EXERCISE 1.2 *What is the Larmor frequency, v_{Larmor}, at which the NMR process takes place for a free proton?*

EXERCISE 1.3 *What is the conceptual difference between the two forms of Equation* (1.2c)*?*

The essential Larmor equation for isolated protons is

$$\boldsymbol{v}_{Larmor}[\text{MHz}] = [42.58\,(\text{MHz/tesla})] \times B_z[\text{T}] \quad (\textit{free protons}), \qquad (1.3)$$

describes the condition under which RF photons from a transmitter will be absorbed by tissue protons and induce nuclear spin transitions (both up and down). Like the Bohr atom, the notion is conceptually and mathematically uncomplicated, yet it is still solid, even if not derived here in a quantum mechanically rigorous manner. In any case, the up-down space quantization constraint is powerful enough for the approach to lead to this fundamental result.

EXERCISE 1.4 *What is the Larmor frequency for protons in a 1.5 T main magnetic field? 3 T? 7 T?*

MRI of a 1D phantom

We can advance from NMR of tissue in a single voxel, at a single point in space, to MRI throughout a region with this spin-up/spin-down model. Consider here a 1D phantom consisting of a single row of voxels lying along the ***x***-axis and containing different amounts of water (Figure 1.3a). The trick is just to establish a gradient magnetic field, $\boldsymbol{G_x}$, that varies along the ***x***-direction,

$$G_x \equiv \partial B_z / \partial x. \tag{1.4a}$$

The *direction* of the gradient magnetic field itself always points 100% *upward* everywhere, but its magnitude is designed to increase linearly with x-position,

$$B_z(x) = B_0 + G_x x, \tag{1.4b}$$

where $\boldsymbol{B_0}$ is the very strong (1.5 or 3 tesla), uniform field from the MRI instrument's main magnet.

EXERCISE 1.5 *Find an expression for the frequency at which the protons in the voxel at position* ***x*** *of a linear phantom resonate.*

This elementary generalization of the Larmor equation provides the critically important prescription for connecting a measured reading of $\nu_{\text{Larmor}}(x)$ to the corresponding value of $\boldsymbol{B_z}(x)$. And once the precise magnitude of $\boldsymbol{G_x}$ has been established and is routinely checked, knowledge of the local $\boldsymbol{B_z}(x)$, in turn, gives up voxel position, x. Now, with the location of each voxel and a measurement of the RF signal strength from it, it

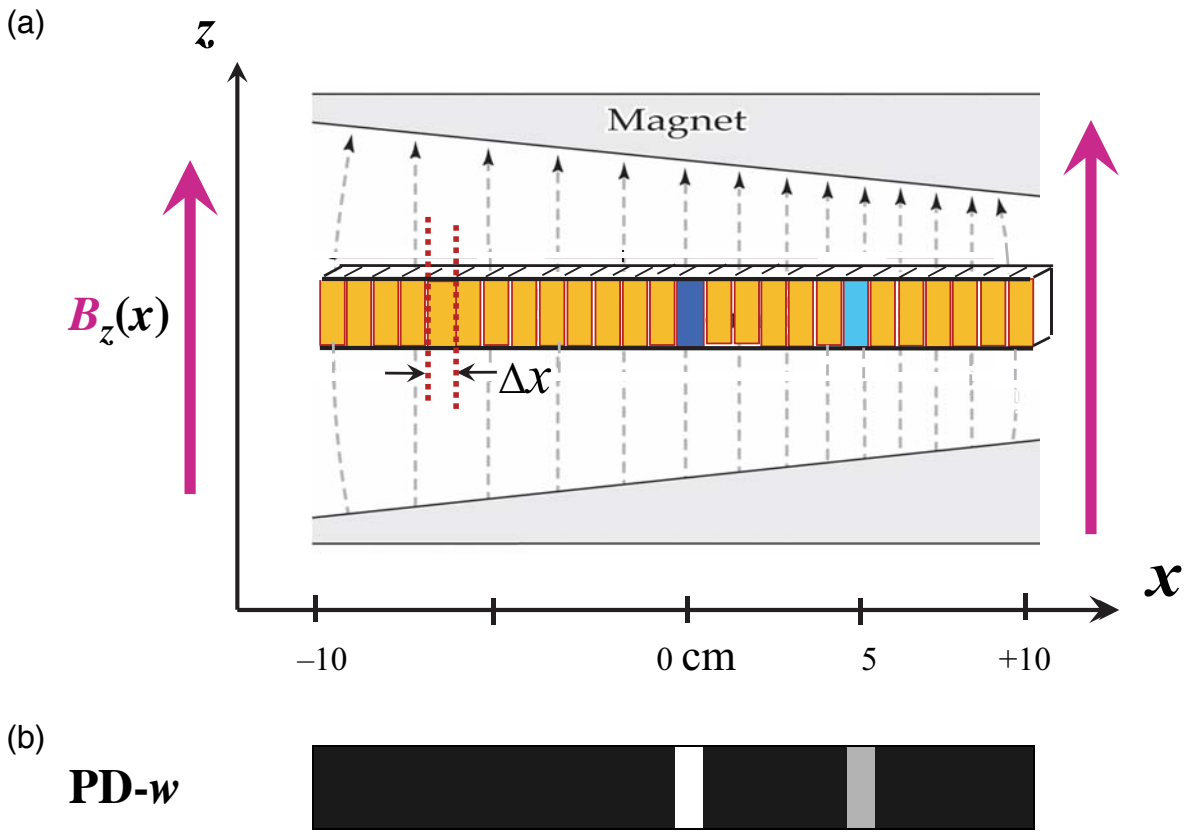

Figure 1.3 This 1D phantom consists of a row of small, hollow chambers, all of width Δx. (a) The one at x = 0 cm contains twice as much water as that at 5 cm, and the others are empty. The main magnetic field points upward along the z-axis at each chamber, but the x-gradient component causes the strength of the *net local* field at each voxel, $\boldsymbol{B_z}(x)$, to increase linearly with position x. Field strength increases as the dashed field lines come closer together. Each of the two water samples undergoes NMR at a different, but precisely measurable frequency. This is an encoding technique that allows determination of voxel position along the x-axis (b), which makes possible the creation of a MR image of proton density (PD) along the phantom. The greater the PD in a voxel, the brighter the pixel shines on the display.

is but a hop, skip, and jump to determining the spatial distribution of *proton density* (PD) within a one-dimensional patient lying along the *x*-axis—which amounts to creating an honest-to-goodness 1D PD MR image (Figure 1.3b). By convention, the greater the PD in a voxel, the brighter the pixel is made to be on the display.

Second picture of NMR: Classical (magnetization precessing in x-y plane)

The other general didactic technique for introducing the NMR phenomenon, the so-called *classical* picture, can actually be derived fully and rigorously from QM theory. It focuses on the composite *nuclear magnetization*, $\boldsymbol{m}(\boldsymbol{r}_j, t)$, the overall magnetic field produced by the tissue protons in the j^{th} voxel at position $\boldsymbol{r}_j$ in 2D or 3D real space:

$$\boldsymbol{m}(\boldsymbol{r}_j, t)\text{: at position } \boldsymbol{r}_j \text{ in 2D- or 3D-space}$$

And despite its quantum mechanical roots, the QM *expectation value* of the time-dependent magnetization, $\langle \boldsymbol{m}(\boldsymbol{r}_j, t) \rangle$, ends up behaving entirely *classically*, governed by the *Bloch equations*, in complete agreement with Newtonian dynamics.

When in a strong magnetic field, the component of the magnetization in the $\boldsymbol{j}^{\text{th}}$ voxel that inhabits (at least temporarily) the ***x-y*** plane normal to $\boldsymbol{B}_z$, namely $\boldsymbol{m}_{xy}(\boldsymbol{r}_j, t)$, will *precess* about it, quite like a toy top or a gyroscope in a gravitational field (Figure 1.4a). (For both proton and gyroscope, the rate of precession increases linearly with field strength.) This rotation of $\boldsymbol{m}_{xy}(\boldsymbol{r}_j, t)$ about $\boldsymbol{B}_z$ happens at the same Larmor frequency as was obtained from the spin-up/spin-down model (Exercise 1.2). Meanwhile, the component of the voxel magnetization that lies along $\boldsymbol{B}_z$ and the *z*-axis, $\boldsymbol{m}_z(\boldsymbol{r}_j, t)$, does not change (unless outside factors such as RF pulses or *spin-relaxation* processes are at work conspire to disrupt the situation). Hereafter we will adopt the ***r*** notation or the *j*, but not both, unless necessary for book-keeping purposes.

The classical picture plays an essential role in discussing the T2 relaxation process, and also the various sequences of RF pulses and gradient magnetic fields that generate signal and contrast in clinical MRI, such as those of the *saturation-recovery*, *spin-echo*, and *gradient-echo* techniques.

The classical approach is conceptually very different from the quasi-QM, and the two are mutually

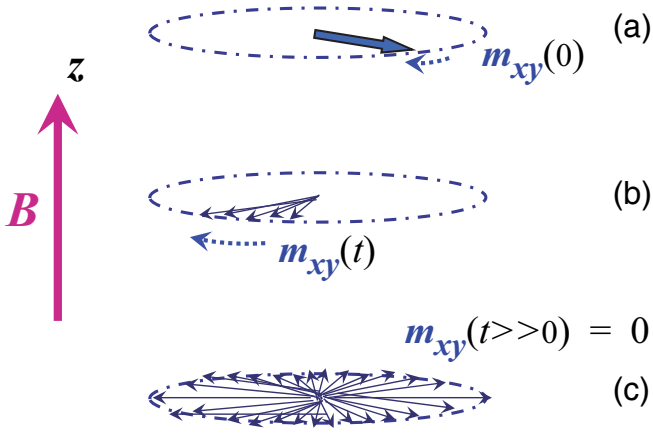

Figure 1.4 The 'classical' view is clearly incompatible with the 'quasi-QM'. (a) The magnetization of a cohort of protons, $\boldsymbol{m}_{xy}(t)$, starts out precessing like a single, narrow vector in the plane transverse to $\boldsymbol{B}_z$. (b) Over time, the protons precess at slightly different rates because of minute differences in their local environments, and they begin to lose phase coherence. The *transverse magnetization* spreads out and diminishes at the rate 1/T2, as $e^{-t/T2}$. (c) After a period several times the tissue's *transverse* or *spin-spin relaxation time*, T2, the protons will be pointing every which way, the sum of their spin vectors will be zero, and $\boldsymbol{m}_{xy}(t \gg T2)$ will vanish.

incompatible, as will be demonstrated later. If you try to combine them, you inevitably end up in trouble. A Sunfish sailboat and a Corvette convertible can each get you from here to the other side of the lake, but you won't get far if you try to fuse the two. The quasi-QM picture has the spin axes of protons pointing up or down in it, while the classical picture has them lying in the ***x-y*** plane and precessing about the *z*-axis—both obviously cannot hold at the same time, an impossibility. To maintain your sanity, don't try to figure out how both can be going on simultaneously, just accept the mystery of it as just being so. More later.

But while seemingly inconsistent, the two models are complementary to one another. In fact, each can be valuable in the right context. But avoid trying to think about NMR with both pictures at the same time. Doing so leads only to weeping and wailing and gnashing of teeth. So just don't try it!

Proton spin relaxation

As the theory and practice of NMR evolved, physicists undertook a second main line of inquiry into the interactions of a nucleus with its environs, namely the *spin-relaxation* mechanisms. The two most important of

these are nuclear *longitudinal spin relaxation* (parameterized by the relaxation time T1) and nuclear *transverse spin relaxation* (T2). These, along with the proton density of the tissue contributing to the signal, play fundamental roles in creating the exquisite soft-tissue contrast associated with clinical MRI.

EXERCISE 1.6 *What are some other systems, mechanical or otherwise, that exhibit near-exponential fall-off behavior over time, distance, radiation dose, etc.?*

Perhaps the best way to get into classical resonance is by way of a familiar analogy. After an initial push, a child's swing resonates at its inherent normal-mode frequency (Figure 1.5), as with many other disturbed physical systems. But any of these will dissipate its energy over time, because of frictional or similar effects, and the amplitude of its oscillation will undergo near-exponential relaxation (decay) with a characteristic *relaxation* or *damping time* T.

Longitudinal proton spin relaxation time, T1

Imagine a bunch of identical compass needles fidgeting about on a gently vibrating table, each trying to align along the Earth's magnetic field. In your mind's eye, give the table a hard whack, immediately after which the needles will point randomly in all directions. Now leave it alone again, and the needles will settle down and begin to re-align mostly northward again. The average amount of time this recovery process takes for the ensemble of compasses is the system's relaxation time, $T_{needles}$. It is determined by the strength of the interaction between the field and a needle, by its mass and shape, and by the nature of the dissipative forces present, such as those occurring at the mechanical pivot points where the needle is supported.

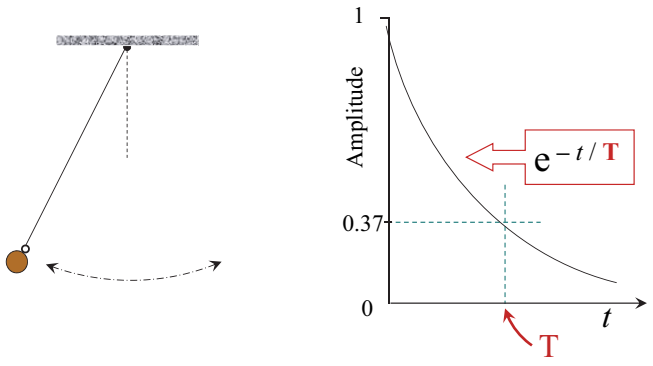

Figure 1.5 A pendulum serves as simple analogue (but not at all a direct model!) for proton resonance and T1 relaxation. The oscillatory motion is affected by friction-like forces that cause it to fall off exponentially over time with a characteristic time 'T.' Analogous phenomena are responsible for the decline of a NMR signal at the rate 1/T1 or 1/T2.

A proton is a fully quantum mechanical entity, of course, but in some ways a cluster of them in a voxel of tissue do behave rather like a bunch of tiny compass needles. They differ, however, in that when a patient lies in the strong magnetic field of an MRI device, a very little bit more than half of them will settle into the lower energy-state. (Here, of course, we're thinking only in terms of the *quasi-quantum mechanical picture*, in which proton spin axes can point only up or down relative to the strong external field!) They don't all end up in the more comfortable and 'natural,' lower-energy alignment along the field, like real compass needles, because magnetic noise from random molecular motions will continuously be knocking their spins both up and down. In a standard 1.5 tesla field, the system achieves a dynamic thermal equilibrium with about five in a million more protons in the lower-energy state, as predicted by Boltzmann statistics. (That may not seem like much, but how many of them are there in a 1 mm^3 voxel?)

You can, with RF excitation at the Larmor frequency, flip some of the lower-energy protons up, and tickle some of the others down, and thereby disturb the equilibrium condition. Do this effectively, and the system eventually has about the same numbers in the two energy levels, a situation known as *spin saturation*. Turn off the RF, and the spins will begin to undergo a kind of spontaneous, thermally induced relaxation process over time analogous to (but in actuality quite different from) that of the compass needles, approximately as

$$[1 - e^{-t/T1}], \qquad (1.5a)$$

with the exponential decay rate of 1/T1. You might assume that it is the photons emitted during this relaxation process that are detected and used to create T1-type MRI images, but that is too rudimentary an explanation. A big issue, indeed, is how to follow all this in time as it happens, a topic to be explored on several occasions along the way.

The time it takes for a voxel-sized cohort of protons to return 63% of the way back toward their equilibrium condition is designated T1, known as the proton spin-lattice or *longitudinal spin-relaxation time*. At t = T1, $[1 - e^{-t/T1}] = [1 - e^{-1}] = 0.63$. But be forewarned —T1 relaxation is only part of what's going on. This argument, by the way, applies to a number of other phenomena that diminish exponentially, such as radionuclides popping off over time, x-ray photons passing deeper into tissue, cells exposed to various amounts of high-LET (linear attenuation coefficient) radiation dose, etc.

Transverse proton spin relaxation time, T2

At the heart of the classical picture of NMR is the notion of the magnetization, $\boldsymbol{m}(t)$, of a voxel of protons precessing in the ***x-y*** plane. This commonly starts out with all the protons aligned together at $t = 0$, so that $\boldsymbol{m}_{xy}(t)$ can be represented as a rotating narrow vector, the arrow back in Figure 1.4a. The individual protons in the voxel, however, sit in magnetic fields that differ slightly from place to place, so that they do not all rotate at exactly the same frequency. For this and other reasons, the orientations of individual spin packets begin to spread out over time as

$$e^{-t/T2}, \tag{1.5b}$$

and they lose their initial phase coherence (Figure 1.4b). The time it takes to fall 37% of the way to this situation is called T2, the spin-spin or *transverse relaxation time*. After several more periods of duration T2, the spin alignments are so dispersed that their vector sum has dropped to near zero (Figure 1.4c) and $\boldsymbol{m}_{xy}(t)$ vanishes.

T1 and T2 clinical images

T1 and T2 are measures of different but overlapping physical processes, such as the rotations of water molecules near a large biomolecule. These times involve the interplay of protons with their biochemical environments in and between the cells of a tissue. T1 and T2 in a voxel are exquisitely sensitive to the detailed nature of friction-like and other interactions of the water and lipid protons with one another and with nearby ions, biomolecules, and membranes. The concentrations and biophysical characteristics of these ions and biomolecules are affected by the type and physiologic status of the cells they constitute—which, in turn, depend on the biological makeup and pathological condition of the tissues. MRI may, therefore, be able to distinguish not only between histologically different tissues, but even between normal and unhealthy regions of the same tissue.

T1 and T2 can be assessed point by point throughout a portion of the patient, in effect, and utilized to create two related but separate kinds of medical images. Through selection of the operating parameters of the MRI device, it is a straightforward matter to display spatial variations in T1, T2, and a range of other clinically revealing tissue characteristics. Put another way, the numerous types of MRI *contrast*, arising from and reflecting separate physical and physiological processes, are obtained with distinct operational settings of the device (sequences of RF and gradient-field pulses, echo time TE, repetition time TR, etc.)

With the widely employed *spin-echo pulse sequences*, the proton MRI signal strength, $s(x,t)$, from the voxel at position x commonly decays through spin-relaxation mechanisms approximately as

$$\begin{aligned} s(x,t) \;\propto\; & PD(x)\times[e^{-2\pi i\nu_L t}] \\ & \times[1-e^{-TR/T1(x)}]\times[e^{-TE/T2(x)}] \end{aligned} \tag{1.6a}$$

PD($\boldsymbol{x}$) is the proton density for the voxel at x, $\nu_L(x)$ the Larmor frequency there, and T1(x) and T2(x) are the two principal spin-relaxation times.

If given the value of $s(x_j, t)$ over time for the voxel at each position x_j, it would be a simple matter to extract and map PD(x), T1(x), and T2(x) throughout the patient. Regrettably, an MR device does not detect individual signals from all the voxels separately, but rather only their superimposed, summed value:

$$S(t) \;=\; \Sigma_j\, s(x_j,t)\,. \tag{1.6b}$$

Much of this book will explore the physical origin, meaning, and analysis of this equation, and of the three clinically important tissue parameters—PD, T1, and T2—and related matters. The mathematical process of separating $S(t)$ into its (thousands of) constituent parts $\{s(x_j, t)\}$ is known as *MR image reconstruction*. A very simple example of this appeared in connection with Figure 1.3

The above has been a rapid sketch of some central aspects of NMR and MRI. The following chapters will

explain and discuss in detail what has been noted so briefly here, starting over at the beginning.

1.2 Uniqueness of MRI

MRI can do much of what CT does, but it is much better at defining the anatomy and finding pathologies in soft tissues. Similarly, it can reveal much of what can be found with nuclear medicine, ultrasound, and other modalities. But there are also valuable studies that only MRI can carry out.

MRI reflects primarily upon the interactions of water and lipids with the biomolecules that happen to be present within and between the cells of tissues. T1- and T2-imaging are powerful because they provide forms of image contrast, based on those interactions, that are altogether different from those of other modalities—ones that are sensitive, in particular, to differences in soft tissue types and that correlate with specific pathologies. As medical physicists, computer scientists, and others continue to provide technical improvements at a rapid clip, the transfer of these evolving technologies to the clinic will open new areas of medical research and, thereafter, of widespread application.

One area of significant clinical growth potential in MRI is in the prediction and monitoring of response to treatment, whether radiation therapy, chemotherapy, local heat ablation with US, gene therapy, or whatever. In cancer therapy, for example, ionizing radiation and certain tumoricidal drugs are relatively ineffective on tumor cells that are poorly oxygenated. Indeed, the most radio-resistant cells are commonly those inhabiting a barely viable hypoxic rind between active tumor, on the outside, and necrotic tumor cells within that have died from anoxia. MRI may well be able to reveal whether a pharmaceutical intended to promote angiogenesis in that rind, or to facilitate the perfusion or diffusion of water or oxygen into it (which may render it more radiation-sensitive), will be successful on a specific patient. Likewise, following the administration of a drug or dose of radiation, MRI and perhaps MR spectroscopy can assess the degree to which the opening or proliferation of blood vessels has increased the oxygen level in hypoxic regions and, therefore, the likelihood of destroying the tumor. These are but two out of countless examples of image-guided therapy (involving MRI alone or in collaboration with other modalities, e.g., PET) that either already exist or are forthcoming.

1.3 A Real MRI Case Study

A female associate professor of genetics experienced erratic diffuse headaches that responded to an Advil or Tylenol. The headaches were mild but still a little disruptive, so after several months she turned to her general practitioner. She presented as a healthy 52-year-old in no apparent distress apart from mild hypertension that was controlled by medication. She followed a good diet and exercised moderately several times a week. Other aspects of her physical examination were unremarkable and, in particular, a neurological examination revealed no deficits. She claimed to be happily married to her best friend and reported no major stresses or anxieties, apart from those arising from rearing two independent and adventurous teenage daughters.

Computed tomography (CT)

Uncomfortable with the duration of the problem, her internist ordered a CT scan of the brain at the local clinic. The results were suggestive of an irregularity in the right posterior temporo-occipital region, partially replacing some of the occipital horn of right lateral ventricle. He felt that an MRI head study could provide better information.

The next day she and her husband drove a half hour to one of her university's teaching hospitals. In her haste at home, she misplaced the DVD of the CT study. After her check-in at the medical center, however, all of her subsequent images, along with lab results and other medical records, were stored safely and kept available for immediate retrieval on the Department of Radiology's *Picture Archiving and Communications System* (PACS).

MRI: T1-w, T2-w, and FLAIR imaging

Although not available, the CT had already performed an invaluable service by drawing attention to the possible irregularity. In any case, the MRI studies would be more revealing of soft-tissue problems. The patient underwent a number of standard MR studies, including the gathering of T1-weighted and so-called FLAIR images (Figure 1.6).

The T1-*w* image supported the CT report, and also noted the extension of a well-circumscribed 1.7×1.1 cm^2 lesion to the lining of the occipital horn of the

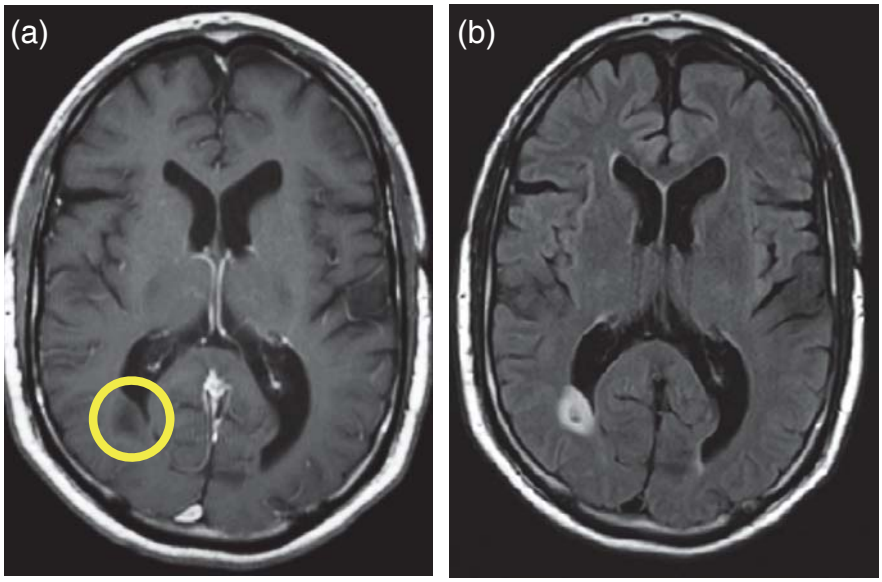

T1-*w* with Gd T2-*w* FLAIR

Figure 1.6 Two MR images of the same thin (1 mm), transverse slice. As with CT, a transverse MRI scan looks upward from the feet. (a) The T1-weighted study reveals a right posterior temporo-occipital lesion adjacent to occipital horn of the right lateral ventricle. Injection of a gadolinium-based MRI contrast agent, as shown here, made no difference visually from an earlier scan obtained without the contrast agent, suggestive that the blood-brain barrier had not (yet) been breached by a growing tumor. (b) The FLAIR (*FLuid Attenuation Inversion Recovery*) study provided different but complementary clinical information. Here signals from *cerebralspinal fluid* (CSF) and other fluids are suppressed, yielding a somewhat different type of MRI contrast, one that better demonstrates the lesion, which is now hyperintense. [*Courtesy of Charles Smith, Peter Hardy, David Powell, University of Kentucky MR Imaging and Spectroscopy Center (MRISC)*].

right lateral ventricle. The absence of bilateral symmetry of the brain was striking, but there was no midline shift or hydrocephalus. The T1-*w* scan was then repeated following the injection of 20 ml of gadolinium (Gd) contrast agent, and little change occurred. Higher-grade neoplasms in the brain are more likely to disrupt the blood-brain barrier, and are thus associated with more avid contrast enhancement. The failure of the region to noticeably take up the agent implied that the lesion was probably not a high-grade neoplasm, a hopeful sign.

A FLAIR image (*FLuid Attenuation Inversion Recovery*) is similar, but suppresses signals from aqueous fluids. In the brain, for example, it eliminates much of the appearance of *cerebrospinal fluid* (CSF), facilitating a better evaluation of the surrounding edema, as well as enhancing lesion conspicuity (Figure 1.6b). The reading radiologist felt that the image indicated a lower-grade glioma protruding into the ventricle, or possibly (although less likely) a tumor-like demyelinating lesion. (A glioma is a common type of tumor that occurs in glial cells, most frequently of the brain; the primary job of these cells is to nurture and maintain neurons, but researches have recently found that they also play a role in neuron functionality.) He also reported several small point-like T2 signal abnormalities scattered throughout the subcortical white matter of the cerebral hemispheres, possibly representing chronic small-vessel blockages or conceivably further areas of neural demyelation.

Magnetic resonance spectroscopy (MRS)

The gold standard in identifying a tumor is a biopsy (physically sampling and microscopic analysis of the tissue). But MRI can provide, in addition to images, quick and non-invasive preliminary information regarding tissue pathology by means of an advanced procedure known as *MR spectroscopy* (MRS).

The Larmor frequency of a proton is determined precisely by the exact magnetic field it experiences. The electrons circulating throughout a biomolecule themselves create a weak magnetic field, and this will affect the magnetic field seen by its tissue protons at various locations. This results in parts-per-million *chemical shifts* in the resonance frequencies of the protons in different molecular surroundings. Then Equation (1.3a) should be modified, if the protons are in a uniform external magnetic field B_0, as

$$\nu_{Larmor} = (\gamma / 2\pi) \times B_0 (1 + \sigma), \qquad (1.7)$$

where the *chemical shift coefficient*, σ, for a particular proton is strongly dependent on the details of its unique molecular environment. This may seem a little like the proton density imaging of Figure 1.3, but here the Larmor frequency is being shifted by the field from orbit-

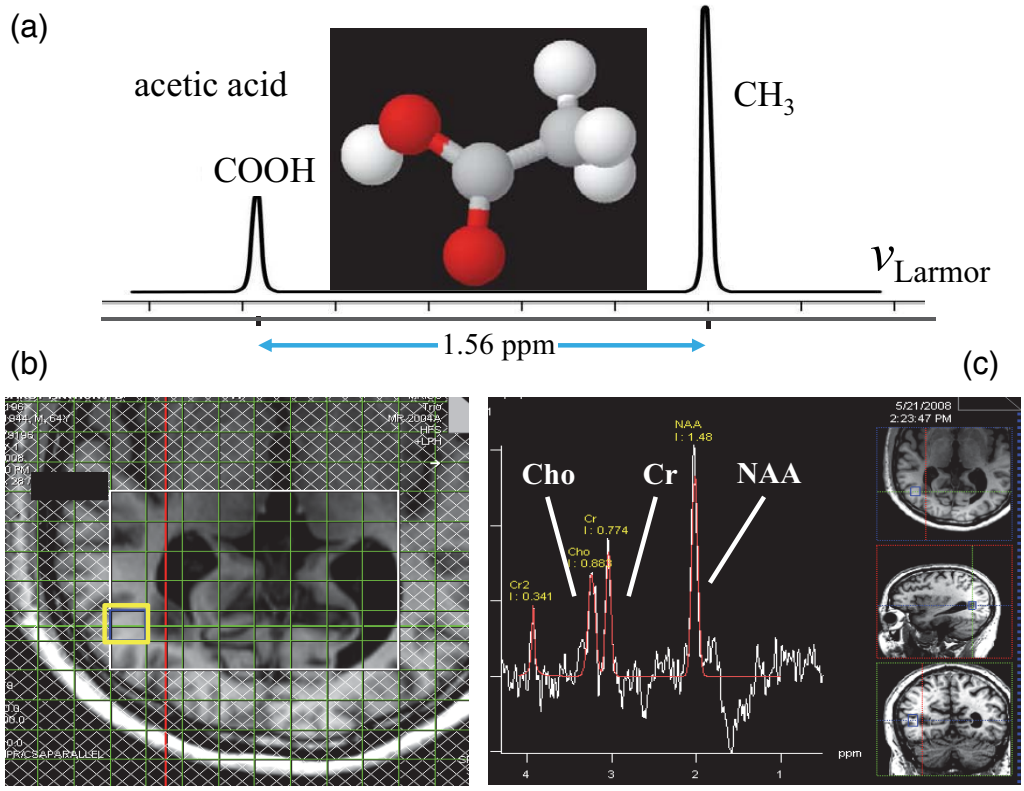

Figure 1.7 An MRS spectrum (a) reflects the uneven circulation of electrons within a molecule (acetic acid) that give rise to small variations in *local* magnetic field, hence in parts per million (ppm) *chemical shifts* in proton Larmor frequency. (b) Tissue just outside the patient's lesion (yellow box) yields a normal MRS spectrum. The spectrum from the lesion itself appears nearly identical, (c) but its higher Cr/NAA and Cho/NAA ratios are characteristic of a glioma.

ing molecular electrons, not by an externally applied gradient field.

The proton nuclear magnetic resonance spectrum of the simple acetic acid (CH_3COOH) molecule, for example, appears as two distinct MR peaks, both very close in resonance frequency to that of a free proton. They are separated by a 1.56 parts per million (ppm) chemical shift in the Larmor frequency, indicating the two slightly different local magnetic fields that the protons can feel (Figure 1.7a). One of the resonance lines is three times the other in amplitude: the three protons within the methyl (CH_3–) group all experience the same swirl of electrons and identical surroundings. The electron flow within the acid (–OOH) group, on the other hand, is different, and its single proton resides in a slightly lower local field.

Protons in molecules imposing a chemical shift are usually too few in number, and with too small a shift, to be seen in standard MRI images, other than lipids. But an MRS instrument combines exceptional homogeneity of the external field with the excellent RF frequency-resolution of an NMR spectroscope, so that protons in different molecular structures can often be distinguished. This allows *in vivo* examination of small, well-localizable volumes of soft tissues, and the spectra obtained may lead to the identification of certain irregularities.

MRS is capable of performing nuclear resonance spectroscopy on small, multi-voxel blocks of tissues at specific locations within the body. For tissues away from the lesion (Figure 1.7b,c) the proton spectra for N-acetylaspartate (NAA), creatine and phospho-creatine (Cr), and choline (Cho) appeared normal. The lesion itself, however, reveals a statistically significant irregularity in the concentrations (areas under the peaks) of Cr and NAA, relative to that of Cho. The spectral signatures for numerous normal and abnormal tissues have been studied, and the pattern seen here, when combined with the imaging information, is indicative of a glioma, but of indeterminate stage.

Functional MRI (fMRI)

Treatment of a tumor depends on its type, anatomical location, grade (degree of abnormality and growth rate seen under a microscope), and stage (size and degree of spread). In the present case, the lesion's position is such that surgery or radiation therapy might well result in the loss of one of the patient's two fields of vision

(to the left or right). While she could accept that, she made it unambiguously clear that she would not agree to any action that would seriously jeopardize her ability to read; she would prefer to leave the disease untreated and take her chances.

Before proceeding to a needle biopsy—which itself could impose some risk to reading vision—she underwent two noninvasive MRI-based studies that would help to determine the closeness of the apparent tumor to optically active regions. The first was *functional MRI* (f MRI) (Figure 1.8a).

In an f MRI study, a subject is asked to undertake a mental process of some sort, such as repeatedly viewing a visual stimulus or tapping a finger. In the process, associated brain tissues become unusually active and consume extra oxygen, transforming oxyhemoglobin into deoxyhemoglobin there more rapidly than when at rest. These two molecules differ magnetically, and deviations in their balance may produce detectable tissue contrast where a region of the brain is being triggered. You might suspect that the relevant neurons are simply burning more oxygen; that indeed happens but, as will be seen later, the brain is far cleverer than that, and the process is actually more subtle and interesting.

Functional MRI data complement those of PET, which lights up those parts of the brain that happen to be burning excess radio-labeled glucose. Other modalities, like electroencephalography (EEG) and magnetoencephalography (MEG), are also being developed for mapping brain function. Establishing correlations among their results and those of f MRI and PET will greatly enhance the medical value of all of them.

The patient underwent f MRI with two separate sets of periodic stimuli, self-directed finger tapping and visual images. Temporal variations (which is what is of interest here) in the MRI signal are much smaller than the average value of the signal voltage itself, and effective noise-rejection and statistical information-processing programs must be invoked. The finger-tapping task demonstrated robust activation within the associated region of the motor cortex of the cerebral hemispheres. The patient's response to an intermittent visual stimulus is shown here in a thin sagittal slice that passes through the circled lesion; it indicates that one of the optically active regions of the brain (in green) lies adjacent to it, and possibly within it. Damage to it could cause catastrophic sight loss.

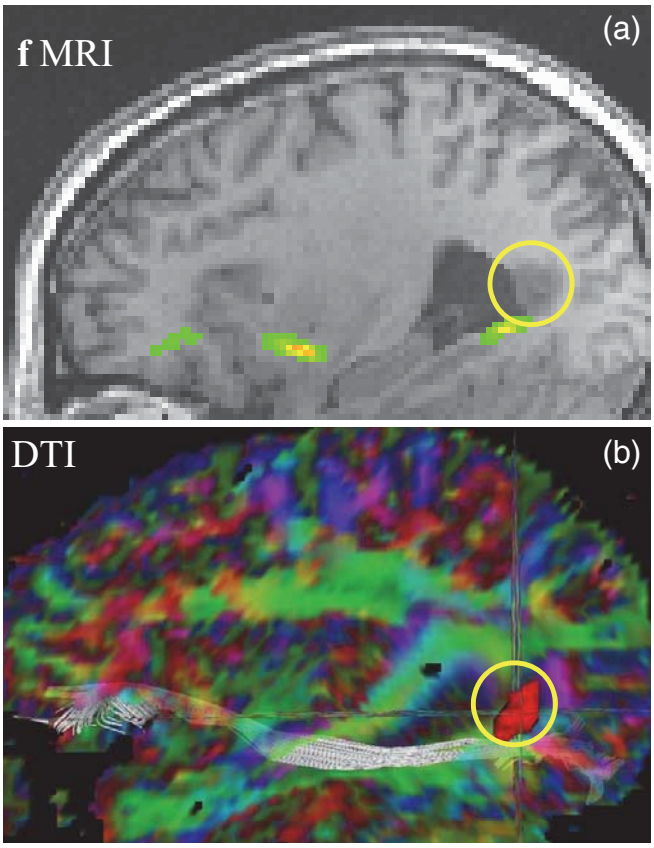

Figure 1.8 MRI for pre-surgical planning. (a) A thin (1 mm) slice sagittal T1-w image with a functional MRI (fMRI) overlay highlights small regions of the brain (yellow-green), near the circled lesion, that respond to a flashing light stimulus. (b) A diffusion tensor image (DTI) further indicates the close proximity of the patient's nerve trunks, the 'optic radiation' (white horizontal strands) to the glioma (red solid). [With thanks to Charles Smith and David K. Powell, University of Kentucky MRISC].

Diffusion tensor MR imaging (DTI)

In view of the rather discouraging f MRI results, it was felt to be worthwhile to carry out a *diffusion tensor image* study, as well. With DTI, contrast arises from the unidirectional *diffusion* of water molecules along the long axons of a nerve trunk, against a background of other water molecules that are diffusing isotropically, thereby bringing the nerve trunks into view. Figure 1.8b. A sagittal, thin-slice DTI corroborated the earlier f MRI finding that the patient's probable glioma lies directly adjacent to, and possibly infiltrating, superior portions of a nerve trunk, the *optic radiation* (the pale horizontal ribbon).

MRI-guided fine-needle biopsy

After viewing all the evidence, and particularly the DTI results, a neurosurgeon felt that with MRI guidance, she could very probably obtain a fine-needle tissue biopsy sample with low chance of damaging the optic radiations. After consulting with her personal physician, the patient agreed to the three-step invasive process.

First, in the operating room and under local anesthesia, a rigid, nonmagnetic frame was screwed firmly into the skull, providing the platform for establishing a fixed Cartesian coordinate system within which to localize the tumor, and later to reach it with a fine biopsy needle.

A separate assembly comprising a box with four flat, transparent walls embedded with weakly magnetic orthogonal positional markers and lines was attached. This provides an orthogonal frame of reference that is visible to the MRI device. Any point within the brain could now be expressed as a set of x-, y-, and z-coordinates relative to the frame, to within one millimeter (Figure 1.9a). MR images were now taken, and from these the neurosurgeon decided where in the lesion she would obtain the biopsy sample, and the path she would follow in getting there.

Then, with the frame still attached rigidly to the skull, the first (MRI-imaging) assembly is removed from it and the second, a stereotactic biopsy needle guidance assembly, is fixed to it (Figure 1.9b). A medical physicist experienced in the use of the equipment made the necessary calculations, based on the images just obtained, and he and the neurosurgeon set the required angles and distance limiters on the mechanical needle-guidance assembly. Soon thereafter, after drilling a small bore-hole in the skull, the surgeon advanced

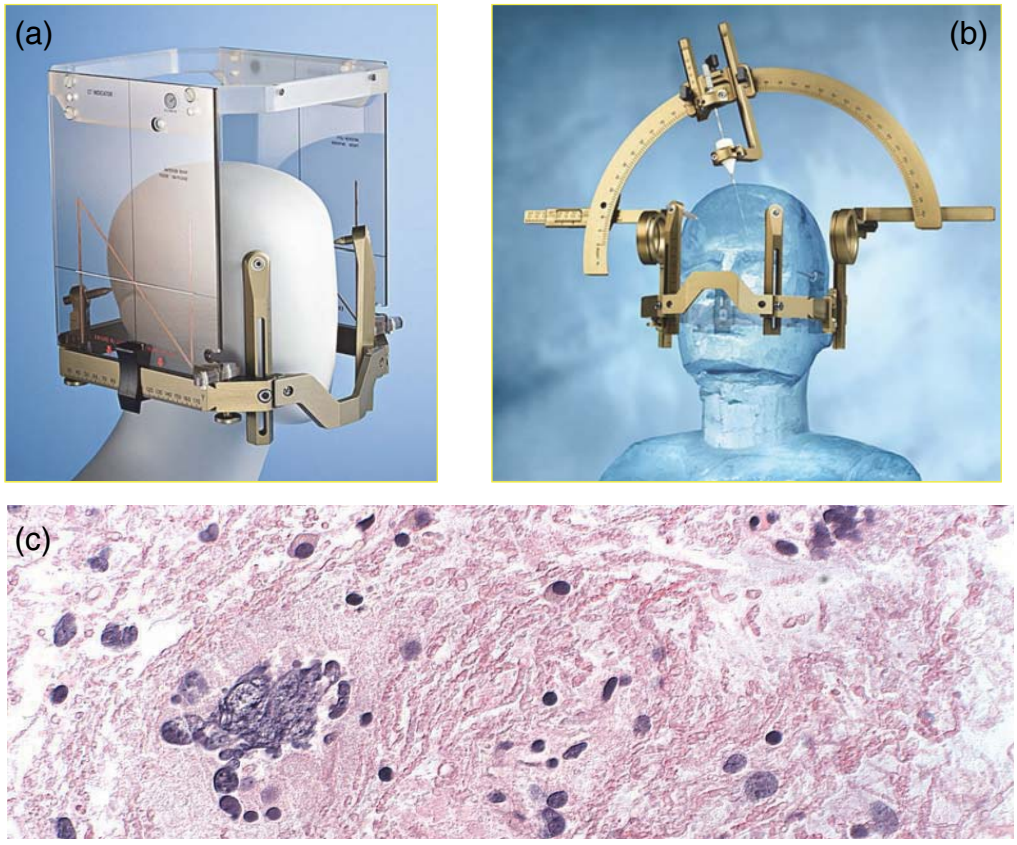

Figure 1.9 A stereotactic fine-needle biopsy device consists of an immobile frame screwed firmly into the scull in the operating room, along with two separate attachments used in sequence. (a) The first of these consists of an array of paramagnetic fiducial markers embedded in plastic planes; these can be read precisely by the MRI device during a clinical study. These make possible accurate localization of a target point within the lesion. (b) Then, with the frame still fastened rigidly to the skull, the first assembly is removed and a second attached. This one can guide insertion of a hollow sampling needle along any direction chosen by the neurosurgeon, such that its tip will end up within 1 mm of the target point. [*Courtesy of Elekta*]. (c) Photomicrograph from one of the biopsy slides. The pathologist reported that the sample collected from this lesion displays scattered and atypical cellular nuclei, suggestive of an astrocytoma, a form of glioma, but of undeterminable grade.

the hollow needle exactly the right distance and obtained the sample without incident.

It was expected that the samples obtained would be definitive, but they were not (Figure 1.9c). The surgeon phoned the patient the evening of the biopsy with a very unoptimistic report from the pathologist: the tissues obtained were equivocal, but suggestive of an advanced, fast-growing high-grade glioma. The patient reacted to the news calmly, her greatest concern being the impact this would have on her husband and daughters, to whom she was devoted. Further examination of the slides a few days later by several other pathologists, remarkably, led to the far less awful prognosis that the glioma may be only of stage-1 or -2, which either can be watched for changes or treated with drugs and radiotherapy with a reasonable chance of control.

Should we try positron emission tomography?

A final diagnostic test was considered, but rejected. Tumors commonly oxidize glucose at a faster rate than do healthy tissues of the same type, and positron emission tomography (PET) is a nuclear medicine modality highly sensitive at detecting excessive cellular uptake and use of it, Figure 0.4b. Sugar molecules are labeled with radioactive fluorine-18, and the injected 18-fluorodeoxyglucose (^{18}FDG) concentrates preferentially in fast-metabolizing tissue, such as neoplasms. The fluorine nucleus decays with the emission of a positively charged *positron*, which travels 1 mm or so and immediately collides with its anti-particle, an electron. The two particles mutually annihilate, giving birth to a pair of 511 keV *annihilation photons*, which fly away from the site of the interaction in almost exactly (to within ¼°) antiparallel directions. If the two are detected simultaneously on the opposite sides of a PET imager, within a tiny time window, they will contribute to the formation of a PET image of the region that had taken up the radiopharmaceutical. Thus, PET is another source of tissue image contrast, but one that exploits the metabolism of radioactive glucose, rather than of normal oxygen, like f MRI.

PET findings might be helpful, such as in finding other lesions in the brain, but it would probably have little or no effect on the patient's treatment, and she and her physicians decided against pursuing it.

Treatment guidance and follow-up

The patient and her physicians, hopeful that the glioma might turn out to be slow-growing or even quiescent, decided that the best course of action was to do nothing. An MRI examination every six months for three years has revealed that, in fact, her tumor was not growing appreciably, and she's still alive and well. In an ironic twist, upon returning home she learned that other residents of her condo were also experiencing headaches. The epidemic ended, as did her own headaches, when the large construction project next door, which frequently produced unpleasant fumes, terminated. So her glioma may well have had nothing at all to do with her symptoms, and was identified by accident.

One area of significant clinical growth potential in MRI is in the prediction and monitoring of response to treatment, whether radiation therapy, chemotherapy, local heat ablation with ultrasound, gene therapy, etc. For example, MRI continued to play a role in treatment of our patient, in part by monitoring any change in the size, shape, or any other aspect in the appearance of the lesion. But some developments in her status might call for additional or alternative treatments.

The purpose of nearly any curative (non-palliative) surgical or other therapy, of course, is to eliminate the problem without causing unacceptable damage to healthy (especially critical) tissues. A procedure similar to that for the fine needle aspiration biopsy (Figure 1.9) can be used to direct a narrow but intense beam of x-rays at the lesion. Linear accelerators (linacs) have been modified to perform microradiosurgery on brain tumors with very small fields and, guided by CT or MRI, with very high precision. Brachytherapy with suitable and meticulously located radioactive seeds might also be appropriate. And for some kinds of surgery, a growing number of institutions have MRI in the operating room in order to aggressively, and more safely, resect the disease. Similarly, chemotherapy drugs can be infused under guided delivery alone or in conjunction with radiation or surgery. How might the general approach described here be applied in other medical procedures [Jolesz 2008]?

In the long run, perhaps the most extraordinary (from our current perspective) clinical advances will arise from ongoing efforts to establish strong linkages among the various forms of physiologic imaging—especially MRI, nuclear medicine, and optical imaging—with genomics, proteomics, molecular biology, and nanotechnology. These fields are just beginning to overlap and unify, yet already they have created novel